

---

# Optimization of Smelting Process of Magnesium Based on Machine Learning

Xin Li<sup>1</sup>, Junhua Guo<sup>2</sup>, Jianglei Fan<sup>1</sup>, Yongbiao Wang<sup>1</sup>, Yanyan Li<sup>3</sup>, Xiaoguang Zhou<sup>4</sup>, Shuxia Tian<sup>1</sup>, Feng Mao<sup>5</sup>, Kunlin Miao<sup>6</sup>, Shizhong Wei<sup>1,7</sup>

1. Zhengzhou University of Light Industry, College of Mechanical and Electrical Engineering, Zhengzhou, 450002, China
2. China Academy of Machinery Zhengzhou Research Institute of Mechanical Engineering Co., Ltd., State Key Laboratory of High Performance & Advanced Welding Materials, Zhengzhou, 450001, China
3. Zhengzhou University of Light Industry, School of Materials and Chemical Engineering, Zhengzhou, 450002, China
4. Northeastern University, State Key Laboratory of Digital Steel, Shenyang, 110819, China
5. Longmen Laboratory, Luoyang, 471000, China
6. Zhengzhou University of Light Industry, School of Computer Science and Technology, Zhengzhou, 450002, China
7. Henan University of Science and Technology, School of Materials Science and Engineering, Luoyang, 471003, China; Henan Engineering Technology Research Center for Wear resistant Materials, Luoyang, 471003, China

Corresponding author: Junhua Guo, [guojunhua92@163.com](mailto:guojunhua92@163.com); Xin Li, [XinLi1384051@163.com](mailto:XinLi1384051@163.com)

Email: Xin Li, [XinLi1384051@163.com](mailto:XinLi1384051@163.com); Junhua Guo, [guojunhua92@163.com](mailto:guojunhua92@163.com);  
Jianglei Fan, [fanjianglei@zzuli.edu.cn](mailto:fanjianglei@zzuli.edu.cn); Yongbiao Wang,  
[wsbiaoyongwang@163.com](mailto:wsbiaoyongwang@163.com); Yanyan Li, [lyzz201@163.com](mailto:lyzz201@163.com); Xiaoguang Zhou,  
[xiaoguangzhou@126.com](mailto:xiaoguangzhou@126.com);

Shuxia Tian, [tiansx@zzuli.edu.cn](mailto:tiansx@zzuli.edu.cn); Feng Mao, [maofeng718@163.com](mailto:maofeng718@163.com);  
Kunlin Miao, [miaokl97@163.com](mailto:miaokl97@163.com); Shizhong Wei, [wsz@mail.haust.edu.cn](mailto:wsz@mail.haust.edu.cn)

**(Received 14 October 2025; Accepted 30 April 2026)**

## Abstract

The traditional magnesium reduction process consumes a significant amount of energy, which contradicts China's green and low-carbon development goals. Therefore, exploring more energy-efficient methods is crucial for environmental protection. The reduction rate of magnesium is influenced by several factors, including gas flow rate, briquetting pressure, ferrosilicon content, reduction temperature, and reduction time. In this manuscript, data analysis utilizing a machine learning algorithm: support vector machine (SVM)—was employed to predict the magnesium reduction rate. Given that energy-saving processes are a primary objective for enterprises, the processing was optimized using the particle swarm optimization (PSO) algorithm based on the SVM model, while maintaining a constant magnesium reduction rate. This optimization aims to reduce energy and gas consumption during the magnesium smelting process.

---

Experimental verification of the magnesium reduction rate under the optimized processing conditions demonstrated that the application of machine learning algorithms can lead to resource savings in the magnesium reduction process. To further evaluate the environmental benefits of the optimized process, a Life Cycle Assessment (LCA) focusing on energy consumption and carbon dioxide (CO<sub>2</sub>) emissions was conducted. The LCA results indicate that the optimized process significantly reduces the life cycle energy consumption (reduced by 5.33%) and CO<sub>2</sub> emissions (reduced by 3.63%) compared with the initial process, providing precise environmental performance data for the promotion and application of magnesium alloys in lightweight structures.

**Keywords:** Machine learning; Magnesium; Reduction rate; Intelligent process optimization

## 1. Introduction

Magnesium and its alloy systems have achieved extensive application across aerospace, automotive, electronic communication, materials metallurgy, and diverse other industrial fields, owing to their superior physicochemical properties [1-3]. They also hold significant utility as biomedical materials and hydrogen storage substrates [4-6], presenting promising market prospects. As a lightweight functional material, magnesium and its alloys are poised to play a crucial role in advancing green, low-carbon, and high-quality development initiatives. However, the increased energy consumption during the reduction process, the need for special protective atmospheres during casting processing, the relatively low mechanical properties, the difficulty in preventing corrosion of magnesium alloys, and their electrode potential being the lowest among metallic materials. They are prone to corrosion during use. Therefore, it is of great significance to study and reduce the energy and gas consumption in magnesium reduction process for magnesium and its alloys.

Two principal technologies dominate global magnesium extraction: electrolytic processes and magnesia thermal reduction methods. In China, primary magnesium production primarily relies on the Pidgeon process, which contributes approximately 80% of the world's total magnesium output [7]. Classified as a silicothermic reduction technique, this process involves reducing magnesium oxide under high-temperature and vacuum conditions. Despite its operational simplicity and flexibility, growing environmental awareness has brought to light inherent drawbacks, including discontinuous operation, extended production cycles, and substantial pollutant emissions [8-10]. Material balance calculations reveal that producing 1 ton of magnesium via the Pidgeon process generates 5-6 tons of waste residues and nearly 5.0 tons of carbon dioxide from carbonate decomposition, with energy consumption equivalent to roughly 10 tons of standard coal. To mitigate energy usage and enhance production efficiency in silicothermic magnesium extraction, continuous innovations and practical applications in magnesium production technology have emerged. Notable examples include the Mintek Thermal Magnesium Process (MTMP) [11], which employs DC open-arc metallothermic smelting for calcined dolomite at atmospheric

---

pressure and temperatures ranging from 1923 K to 2023 K. The one-step process [12] and integrated calcination-reduction magnesium production process [13], both of which eliminate the cooling stage following high-temperature calcination. And the microwave-assisted Pidgeon process [14], which utilizes microwave heating to boost heat transfer efficiency and shorten the reduction cycle. The carbothermic process [15,16] has long been recognized as the lowest-cost magnesium smelting technology, yet the occurrence of reverse reactions during reduction has precluded its industrial-scale application.

Contemporary research endeavors in magnesium extraction predominantly rely on magnesium oxide and aluminum as key feedstocks. This conventional workflow necessitates first calcining magnesite, followed by cooling the high-temperature magnesium oxide to ambient temperature. The cooled magnesium oxide is then blended with aluminum, compacted into pellets, and reheated to the required reduction temperature. This sequential process not only results in significant heat and energy wastage but also diminishes the reactivity of magnesium oxide due to its hygroscopic nature. Furthermore, the vacuum environment traditionally required for magnesium production restricts mechanization and automation levels, making continuous operation challenging to achieve. In response to these constraints, drawing on the concept of a gas-driven low-pressure atmosphere [17-19]—wherein a flowing inert gas supplies the necessary environment for magnesium pellet production—and from the perspective of optimizing the comprehensive utilization of low-grade magnesite resources, a novel silicothermic process for the direct reduction of low-grade dolomite to magnesium under flowing argon has been proposed. In this innovative approach, dolomite and ferrosilicon are directly mixed and pelletized, followed by calcination at a specific temperature. Post-calcination, the high-temperature pellets are directly introduced into the reduction stage, with the entire process conducted under a flowing inert gas atmosphere. Magnesium vapor generated during the reaction is carried away from the reaction zone by the flowing inert gas and condensed into crystalline form in a dedicated condensation zone. This integrated process preserves the high reactivity of magnesium oxide produced from dolomite calcination, thereby improving the magnesium oxide reduction rate. It also enables magnesium production under atmospheric pressure, facilitating continuous operation and enhancing overall production efficiency. However, the smelting process of magnesium needs consume expensive inert gases, which is not conducive to resource conservation. If the traditional experimental method is used to study the magnesium smelting process to save energy and gas consumption, a large number of experiments are required, which will lead to more resource consumption and is not conducive to environmental protection. Notably, the environmental performance of magnesium smelting processes is a key factor restricting the promotion of magnesium alloys in lightweight structures. As emphasized by relevant studies, Life Cycle Assessment (LCA) focusing on energy consumption and CO<sub>2</sub> emissions is an effective tool to evaluate the environmental sustainability of materials and processes [20,21]. Similar to the application of high-strength steel in automobiles—where end-users require both performance data and carbon emission information to conduct life cycle evaluations of automotive components—magnesium

---

alloy producers also need to provide clear environmental performance data (e.g., energy consumption and CO<sub>2</sub> emissions) to support the downstream application of lightweight magnesium components. Therefore, integrating LCA into the optimization of magnesium smelting processes is crucial to verify the environmental benefits of energy-saving measures and promote the large-scale application of magnesium alloys.

With the development of machine learning (ML) in the field of materials metallurgy [22], it provides a new idea for the optimization of magnesium smelting process. ML can master the information in the data through algorithms, so as to achieve high-precision prediction of mechanical properties or target variables, even process optimization. Among many ML algorithms, SVM was developed based on statistical learning theory. Its basic principle is to find the optimal linear function in the feature space to minimize the difference between the predicted value and the actual value in the whole data set. Various material properties were successfully predicted by the SVM model [23-26]. For example, based on a much smaller database, the corrosion rate of 3C steel in different environments was precisely predicted using an SVM trained on only 46 samples, and the deviation between the predicted and experimental values was less than 0.5  $\mu\text{A cm}^{-2}$ [27]. In addition, SVM was used to predict interphase precipitation particles characteristic values based on 88 samples, on this basis, alloy element content was reduced by using PSO algorithm [28]. These studies show that SVM is suitable for small datasets and nonlinear regression fields, and providing a reference for reducing energy and gas consumption in the smelting process of magnesium.

The kinetics of extracting magnesium from dolomite in a flowing argon atmosphere were investigated in this manuscript. The study examined the effects of gas flow rate, briquetting pressure, ferrosilicon content, reduction temperature, and reduction time on the magnesium reduction rate. Machine learning algorithms were employed to identify methods for reducing energy and gas consumption during the magnesium smelting process, and the optimization results were experimentally validated. Furthermore, a Life Cycle Assessment (LCA) was performed to quantify the energy consumption and CO<sub>2</sub> emissions of the optimized process, providing precise environmental performance data for the downstream application of magnesium alloys in lightweight structures. This integrated approach of "process optimization + LCA assessment" not only verifies the technical feasibility of the proposed method but also highlights its environmental advantages, addressing the core demand for green and low-carbon development in magnesium metallurgy.

## **2. The machine learning process for optimizing the smelting process of magnesium**

To optimize the magnesium smelting process using a machine learning algorithm and to reduce energy and gas consumption, this manuscript presents a flowchart of the

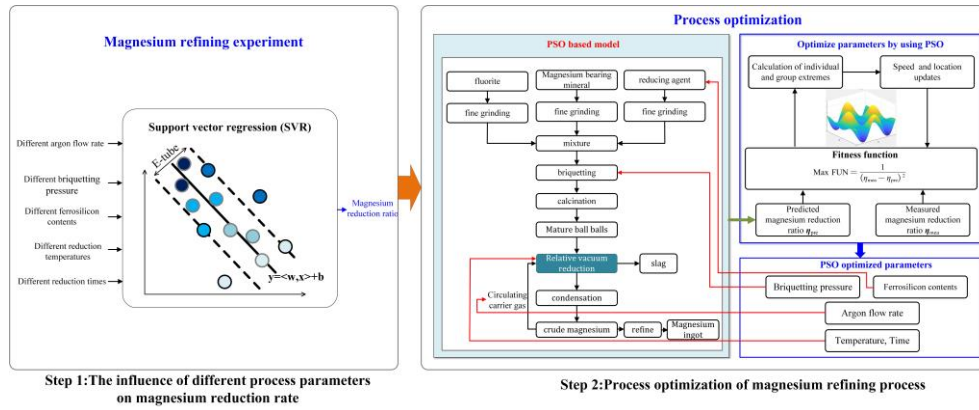


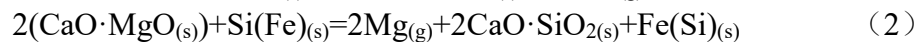
Fig. 1 The flowchart of machine learning

machine learning approach, as illustrated in Fig. 1. Initially, experiments were conducted to determine the effects of various factors, including argon flow rate, briquetting pressure, ferrosilicon content, reduction temperature, and reduction time, on the magnesium reduction rate. A nonlinear mapping relationship model was established using the Support Vector Machine (SVM) model to correlate these factors with the magnesium reduction rate. Subsequently, the Particle Swarm Optimization (PSO) algorithm was employed to optimize the magnesium smelting process, successfully achieving the objective of reducing energy and gas consumption. Finally, the reduction rate of magnesium under the optimized process was validated through experimental results.

## 2.1 Experimental materials and methods

### 2.1.1 Experimental materials

At present, the silicothermic process is primarily employed for the extraction of magnesium in the magnesium smelting industry. The raw material used is dolomite ( $\text{MgCO}_3 \cdot \text{CaCO}_3$ ), which is calcined to produce dolime. This dolime is then mixed with ferrosilicon to facilitate a reduction reaction. The resulting magnesium vapor is condensed and crystallized to yield crude magnesium. The principal reactions occur as described in Equations (1) and (2).



Ferrosilicon alloy, containing 75% to 78% silicon, sourced from Anyang Huatuo Metallurgy Co., Ltd., was selected as the reducing agent for magnesium smelting in this manuscript. During the experiment, the ferrosilicon was crushed and finely ground to a particle size of less than 74  $\mu\text{m}$ . The phase analysis results of the ferrosilicon are presented in Fig. 2. As illustrated in Fig. 2, the primary phase in the ferrosilicon alloy is elemental silicon, with a minor presence of  $\text{FeSi}_2$ , indicating that this ferrosilicon alloy possesses good reactivity. The chemical composition is detailed in Table 1.

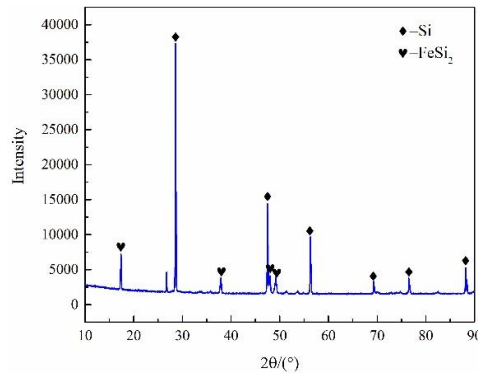


Fig. 2 Phase analysis of ferrosilicon

Table 1 Chemical composition of ferrosilicon alloy

element	Si	S	P	C	Fe
content (mass%)	74.13	0.018	0.031	0.07	≤25.751

## 2.1.2 Experimental methods

By using flowing inert gas to transport the magnesium vapor produced by the reaction away from the reaction zone, the partial pressure of magnesium vapor on the surface of the pellets can be maintained at a level consistently lower than the equilibrium partial pressure of the reaction, thereby allowing the reaction to proceed continuously. The magnesium smelting process involves momentum transfer between fluids. As the inert gas flows over the surface of the pellet, the viscous forces between gases moving at different velocities cause the magnesium vapor particles, which were initially undergoing irregular thermal motion, to be accelerated by the faster-moving inert gas particles. This interaction results in an increase in the momentum of the magnesium particles.

The theoretical schematic diagram of magnesium smelting in a flowing argon atmosphere is presented in Fig. 3. As the inert gas flows over the surface of the pellet, it encounters resistance from both the pellet and the pipe wall, causing the gas to flow in various directions. The magnesium particles, initially in irregular motion, are accelerated by the inert gas, resulting in increased velocities in both the x and y directions. Due to the rapid acceleration of the magnesium particles under the influence of an external pressure head, the dynamic pressure head rises at the moment of acceleration, while the static pressure head remains constant. This leads to a decrease in the static pressure head. Consequently, by utilizing flowing inert gas to exert work on the magnesium particles, their movement speed is enhanced, the dynamic pressure head is elevated, and the partial pressure of magnesium vapor is reduced. In other words, the static pressure head is lowered, placing the magnesium partial pressure on the surface of the pellets in a state that is lower than the equilibrium partial pressure, thereby allowing the reduction reaction to continue.

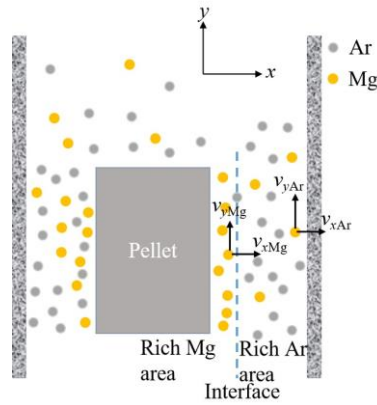


Fig. 3 Schematic diagram of flowing argon atmosphere magnesium smelting theory

A 1:1 mixture of magnesite and calcium carbonate was utilized to replace dolomite in the experiment. This mixture was then combined with ferrosilicon in a stoichiometric ratio. Using 1 mol of MgO as a reference, the ratios were calculated as follows:  $MgO/CaO = 1$  and  $Si/2MgO = M$ . The amount of calcium fluoride added was 3% of the total mass of the raw materials used. The raw materials employed in the experiment, calcium carbonate and calcium fluoride, were both chemical reagents with purities of  $\geq 99\%$  and  $\geq 98.5\%$ , respectively. Consequently, they were regarded as pure substances, and the ingredients were prepared according to this relationship.

The amount of magnesite to be added is calculated as follows:  $W_{\text{magnesite}} = (1 \times 84.31) \div 95.55\% = 88.24 \text{ g}$ .

The amount of ferrosilicon  $W_{\text{Si-Fe}}$  (g) to be added is calculated as follows:  $W_{\text{Si-Fe}} = 0.5 \times 28.09 \div 74.13\% = 18.95 \text{ g}$ .

The amount of  $CaCO_3$  to be added is 100.09 g.

The amount of fluorite ( $W_{\text{fluorite}}$ ) to be added is calculated as follows:  $W_{\text{fluorite}} = (W_{\text{Si-Fe}} + W_{\text{magnesite}} + W_{\text{CaCO}_3}) \times 0.03 = 6.22 \text{ g}$ .

The smelting process of magnesium using magnesite-calcium carbonate as the raw material, along with pellets containing varying silicon content, was investigated in this experiment. Ferrosilicon was added in excess amounts of silicon at 0%, 5%, 10%, 15%, and 20%, corresponding to M values of 1.00, 1.05, 1.10, 1.15, and 1.20. In this study, these pellets were referred to as prefabricated pellets, and the theoretical calculations of the ingredients are presented in Table 2. After the raw materials were shaped through pressing, the prefabricated pellets were calcined at 1273 K for one hour.

Table 2 Theoretical calculation of ingredients

raw material	M	Si-Fe(g)	Magnesium content(%)	Silicon content(%)	Calcination weight loss rate(%)	Magnesium content after calcination(%)
Prefabricated pellets	1	18.95	11.24	6.58	41.22	19.12
	1.05	19.90	11.19	6.88	41.03	18.98
	1.10	20.84	11.14	7.17	40.84	18.83
	1.15	21.79	11.09	7.46	40.66	18.69
	1.20	22.74	11.04	7.75	40.47	18.55

---

### **2.1.2.1 Experimental method for the influence of gas flow rate on the reduction rate of magnesium oxide**

Due to the direct impact of gas flow rate on the reduction rate of magnesium oxide, this section investigates the effect of varying gas flow rates on the reduction rate of magnesium oxide. Previous research [29] indicates that prefabricated pellets demonstrate optimal activity and reaction rates when calcined at 1273 K for one hour. Consequently, during the experiment conducted in a vertical vacuum atmosphere furnace, the pellets were initially calcined at 1273 K for one hour. After this, the crucible containing the pellets was removed from the constant temperature heating zone. Once the furnace reached the designated temperature, the pellets were returned to the constant temperature heating zone. It was ensured that the pellets did not react during the heating phase of the furnace. The fully calcined pellets were then reduced at 1573 K for two hours. The results regarding the influence of different gas flow rates on the reduction rate of magnesium oxide were subsequently obtained.

### **2.1.2.2 Experimental method for the influence of briquetting pressure on the reduction rate of magnesium oxide**

Prefabricated pellets are produced by uniformly compressing dolomite and additives, such as ferrosilicon, into spherical shapes. These pellets must undergo calcination prior to the reduction stage. The calcination process generates CO<sub>2</sub>, which creates voids within the pellets, leading to a reduction in their density. This decrease in density may adversely affect the reduction process. Consequently, this section investigates the impact of briquetting pressure on the reduction rate of magnesium oxide in the silicothermic process. The hydraulic pelletizing equipment was utilized to prepare pellets for the experiment. The pellets, formed by the grinding tool, were cylindrical in shape. The experiment was conducted under various briquetting pressures. When the equipment pressure readings were set at 5 MPa, 10 MPa, 15 MPa, 20 MPa, and 25 MPa, the actual briquetting pressures corresponding to the equipment diameter and pellet diameter were measured at 69.69 MPa, 139.38 MPa, 209.07 MPa, 278.76 MPa, and 348.45 MPa, respectively. In the subsequent sections, the briquetting pressures will be expressed using the equipment readings. The experiment was carried out in a vacuum atmosphere furnace, with prefabricated pellets calcined at 1273 K for one hour and subsequently reduced at 1573 K for two hours. To ensure precise calcination and reduction times during the experiment, the pellets were placed in a constant temperature zone after the resistance furnace was heated to the specified temperature. The effect of varying briquetting pressures on the reduction rate of magnesium oxide was analyzed.

### **2.1.2.3 Experimental method for the influence of ferrosilicon content on the reduction rate of magnesium oxide**

Ferrosilicon, when used as a reducing agent, significantly influences the reduction rate of magnesium oxide. An excessive ferrosilicon content can lead to resource wastage and increased costs in magnesium smelting. Conversely, insufficient ferrosilicon content can adversely affect the thermodynamics of the silicothermic magnesium smelting reaction, resulting in a decrease in Gibbs free energy and,

consequently, a reduced recovery rate of magnesium. Therefore, this section investigates the impact of ferrosilicon content on the reduction rate of magnesium oxide. The molar ratio of Si to 2MgO is denoted as M, with ferrosilicon content represented by this ratio. In the experiment, M values were set at 1.0, 1.05, 1.10, 1.15, and 1.20. Prefabricated pellets were calcined at 1273 K for one hour and subsequently reduced at 1573 K for two hours. The experimental process was conducted in a flowing argon atmosphere with a gas flow rate of 0.2 m<sup>3</sup>/h. The effect of ferrosilicon content on the reduction rate of magnesium oxide was obtained.

#### **2.1.2.4 Experimental method for the influence of reduction temperature and reduction time on the reduction rate of magnesium oxide**

The silicothermic process is an endothermic reaction, meaning that temperature significantly influences chemical reactions. As the temperature increases, the reduction rate accelerates, causing the reaction equilibrium to shift to the right. However, excessively high temperatures can lead to increased process costs, as well as heightened demands for furnace reduction and energy consumption. Therefore, it is essential to control the reduction temperature effectively. Additionally, optimizing the reduction time can greatly enhance production efficiency and reduce costs. This section explores the effects of reduction temperature and reduction time on the reduction rate of magnesium oxide. During the experiment, the flow rate of argon gas was set at 0.2 m<sup>3</sup>/h, the briquetting pressure was maintained at 15 MPa, and the ferrosilicon content (M) was 1.15. The temperature range for the experimental investigation was 1473 K to 1623 K, with a maximum reduction time of 4 hours of insulation. The results regarding the impact of reduction temperature and reduction time on the reduction rate of magnesium oxide were obtained.

After the experiment, X-ray diffraction (XRD, Bruker D8, Germany) and inductively coupled plasma optical emission spectroscopy (ICP-OES, Optima 8300DV, Perkins Elmer, USA) were employed to conduct phase analysis and determine the magnesium content of the cooling slag, respectively. The reduction rate of magnesium is calculated using Eq. (3).

$$\eta_{\text{Mg}} = \frac{m_1 \times \alpha - m_2 \times \beta}{m_1 \times \alpha} \quad (3)$$

Where  $\eta_{\text{Mg}}$  represents the reduction rate of magnesium,  $m_1$  denotes the initial mass of the pellet,  $\alpha$  indicates the magnesium content of the pellet,  $m_2$  refers to the mass of magnesium slag, and  $\beta$  signifies the magnesium content of the magnesium slag.

## **2.2 Establishment of the SVM model for Predicting magnesium reduction Rate**

To reduce energy and gas consumption during the magnesium reduction process, it is essential to establish a model for predicting the magnesium reduction rate. Given the numerous factors that influence the magnesium reduction rate and the non-linear

relationships among them, it is challenging to represent these factors using traditional mathematical models. Furthermore, there is a limited amount of measured data on the magnesium reduction rate. Consequently, it is imperative to develop a new method for accurately predicting the magnesium reduction rate. SVM finds an optimal hyperplane in high-dimensional space to maximize the interval between data points and hyperplane [22], Fig. 1 left. SVM model has the advantages of clear output results, clear boundaries, stable performance of high-dimensional data, small sample robustness, good generalization effect and stable results. Previous researches [23-28] have suggested that the radial basis function (RBF) kernel support vector machine (SVM) model offers significant advantages in the analysis of small datasets and nonlinear regression applications. It effectively captures the nonlinear relationship between the magnesium reduction rate and its influencing factors. The input parameters for the SVM model included gas flow rate, briquetting pressure, ferrosilicon content, reduction temperature, and reduction time, while the output was the magnesium reduction rate. This study utilized 36 data points related to magnesium reduction rates, which were divided into training and testing sets in an 80:20 ratio. During the training of the SVM model, the particle swarm optimization algorithm was employed to optimize the structural parameters ( $c$ ,  $g$ ,  $p$ ) of the SVM. In this paper, Root Mean Square Error (RMSE, Eq.(4)) is used to evaluate the performance of SVM model. The smaller the RMSE is, the higher the accuracy of SVM model is.

$$\text{RMSE} = \sqrt{\frac{1}{n} \sum_{i=1}^n (y_i - \hat{y}_i)^2} \quad (4)$$

Where,  $y_i$  is the measured value,  $\hat{y}_i$  is the predicted value,  $n$  is the sample number.

### 3. Results and Discussion of the SVM Model

Fig. 4 illustrates the comparison between the predicted magnesium reduction rates generated by the SVM model and the corresponding measured values. The predicted values demonstrate a strong correlation with the measured values, exhibiting a root mean square error (RMSE) of less than 2.84%. This indicates that the developed SVM model possesses high accuracy and is suitable for predicting the magnesium reduction rate.

Fig. 5 illustrates the effects of gas flow rate and briquetting pressure on the magnesium reduction rate. It is evident that as the gas flow rate increases, the magnesium reduction rate initially rises gradually and then stabilizes at a relatively constant level. This phenomenon occurs primarily because, at low gas flow rates, an increase in flow enhances the movement of magnesium vapor, leading to a higher magnesium reduction rate. However, once the gas flow rate reaches a certain threshold, excessive flow can lower the temperature of the reduction reaction, resulting in a decreased magnesium reduction rate. Furthermore, it is observed that as briquetting pressure increases, the magnesium reduction rate first rises gradually and then begins

to decline. This behavior can be attributed to the fact that at low briquetting pressures, increasing the pressure reduces the distance between the reducing agent and the raw material. As the reduction reaction progresses, the diffusion distance for atoms decreases, thereby increasing the magnesium reduction rate. However, when briquetting pressure exceeds a certain level, the excessive pressure compresses the distance between the reducing agent and the raw material too much, preventing the magnesium vapor from evaporating, which ultimately reduces the magnesium reduction rate.

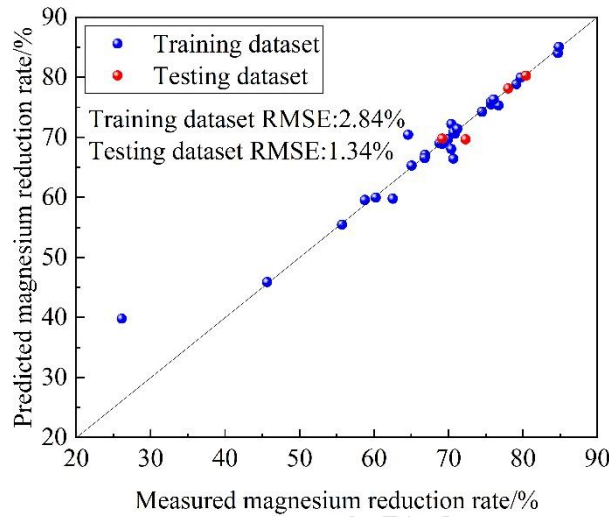


Fig. 4 Comparison between predicted and measured magnesium reduction rate in training and testing datasets

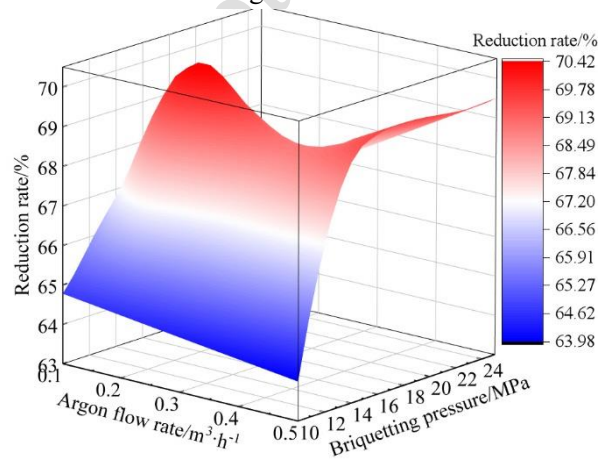


Fig. 5 The influence of gas flow rate and briquetting pressure on magnesium reduction rate

Fig. 6 illustrates the impact of reduction temperature and reduction time on the magnesium reduction rate. It is evident that as both the reduction temperature and reduction time increase, the magnesium reduction rate progressively rises. This phenomenon can be attributed to the fact that higher reduction temperatures and extended reduction times facilitate faster diffusion reactions, resulting in an elevated magnesium reduction rate.

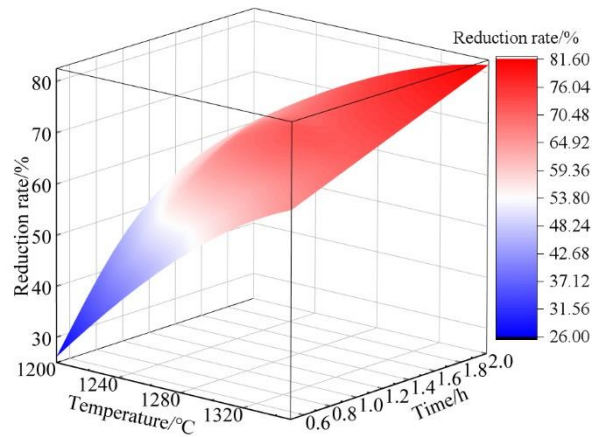


Fig. 6 Effects of reduction temperature and reduction time on magnesium reduction rate

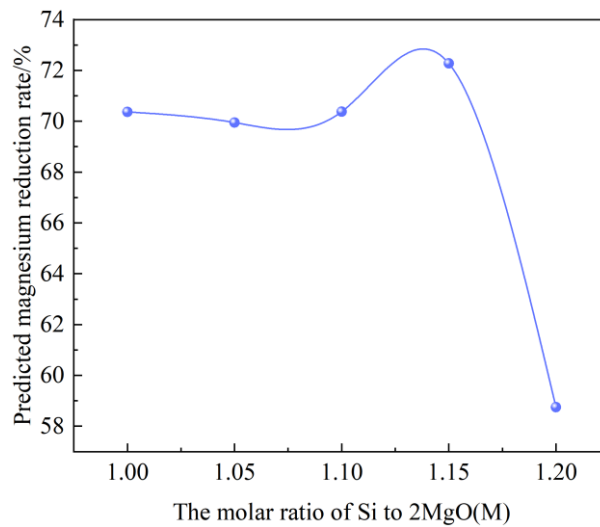


Fig. 7 Effects of ferrosilicon content on magnesium reduction rate

Fig. 7 illustrates the effect of ferrosilicon content on the magnesium reduction rate. It can be seen that with the increase of ferrosilicon content, magnesium reduction firstly increases and then decreases. When M is 1.15, the maximum magnesium reduction rate is 72.28%. This is mainly because when the ferrosilicon content is low, the contact area between MgO and reductant increases with the increase of ferrosilicon content, which accelerates mass transfer and is conducive to the reduction of magnesium oxide. When M is 1.20, MgO and SiO<sub>2</sub> enter the slag to participate in the slagging process without reduction, resulting in waste of reductant and low recovery rate of metal magnesium.

Figs. 5-7 illustrate the effects of gas flow rate, briquetting pressure, ferrosilicon content, reduction temperature, and reduction time on the magnesium reduction rate as predicted by the established SVM model. This prediction aligns with metallurgical mechanisms, indicating that the SVM model is a reliable tool for forecasting the magnesium reduction rate.

---

## 4. Intelligent optimization of the smelting process of magnesium

### 4.1 Process optimization process

To reduce energy and gas consumption during the magnesium smelting process, it is essential to optimize this process. Based on the results of the SVM model presented in Section 3, the magnesium smelting process was optimized using a PSO algorithm, as illustrated in Fig. 1. In designing the fitness function, the objective is to minimize the difference between the measured magnesium reduction rate and the predicted magnesium reduction rate, as expressed in Eq. (5). For the PSO optimization, the population size is set to 20, and the number of evolutionary generations is set to 200.

$$\text{Max FUN} = \frac{1}{(\eta_{\text{mea}} - \eta_{\text{pre}})^2} \quad (5)$$

where,  $\eta_{\text{mea}}$  represents the measured magnesium reduction rate, and  $\eta_{\text{pre}}$  represents the magnesium reduction rate predicted by the SVM model.

### 4.2 Experimentation

The smelting process for magnesium was optimized using the method described in Section 4.1, achieving a magnesium reduction rate of 85%. The initial and optimized magnesium smelting processes are presented in Table 3. Compared to the initial process, the optimized process demonstrates a reduced gas flow rate, decreasing from 0.2 m<sup>3</sup>/h in the original process to 0.16 m<sup>3</sup>/h. Additionally, the magnesium smelting time has been shortened from 4 hours in the original process to 3.72 hours. To verify the magnesium reduction rate under the optimized conditions, magnesium smelting experiments were conducted following the experimental method outlined in Section 2.1. The calculated magnesium reduction rate for the optimized process is 85%, indicating that machine learning algorithms can effectively optimize the magnesium smelting process, thereby achieving significant reductions in gas and energy consumption, which is crucial for resource conservation.

Table 3 Comparison of initial and optimized magnesium smelting processes

process	gas flow rate m <sup>3</sup> /h	Briquetting pressure MPa	Ferrosilicon content/ Stoichiometric ratio	reduction temperature °C	reduction time h	magnesium reduction rate %
Initial process	0.2	15	1.15	1400	4	85
Optimized	0.16	15	1.12	1398	3.72	85

## 5. Life Cycle Assessment (LCA)

### 5.1 LCA assessment scope and goal

The goal of this LCA study is to evaluate the environmental impacts of the optimized magnesium smelting process (based on SVM-PSO) in terms of energy consumption and CO<sub>2</sub> emissions, and to compare it with the initial process. The assessment scope follows the stages of fine grinding, mixture, briquetting, calcination, and reduction in a flowing argon atmosphere. The functional unit is defined as "1 ton of primary magnesium produced", which is consistent with the common functional unit in magnesium metallurgy LCA studies [20], ensuring the comparability of assessment results.

### 5.2 LCA data sources and assessment method

The data required for LCA were collected from two sources: (1) Experimental data from this study, including energy consumption (electricity) and gas consumption (argon) during the optimized smelting process; (2) Literature data for the traditional Pidgeon process [7, 11], including energy consumption (standard coal equivalent), CO<sub>2</sub> emissions from carbonate decomposition and fuel combustion, and other relevant environmental data. The LCA assessment was conducted using the ISO 14040/14044 standards, and the environmental impact assessment was focused on two core indicators: total energy consumption and CO<sub>2</sub> emissions.

### 5.3 LCA Results and Analysis

Table S6 (see Appendix for details) presents the comparison of total energy consumption and CO<sub>2</sub> emissions between the optimized process and the initial process. It can be seen that the total energy consumption of the optimized process is 2971.48 kgce · t<sup>-1</sup> Mg, which is 5.33% lower than that of the initial process. In terms of CO<sub>2</sub> emissions, the optimized process emits 15.428 t · t<sup>-1</sup> Mg, a reduction of 3.63% compared with the initial process, 20% of argon gas consumption compared with the initial process (Table 3). The significant reduction in energy consumption, CO<sub>2</sub> emissions and argon gas consumption is mainly attributed to the optimization of smelting parameters (gas flow rate, reduction temperature, etc.) by the SVM-PSO algorithm, which reduces the energy waste caused by improper parameters and improves the utilization efficiency of raw materials and energy.

These LCA results indicate that the optimized magnesium smelting process

---

proposed in this study has obvious environmental advantages. Similar to the application of high-strength steel in automobiles—where providing carbon emission data for end-users is crucial for automotive lightweight life cycle evaluation—the energy consumption and CO<sub>2</sub> emission data obtained from this LCA study can provide a reliable basis for the promotion and application of magnesium alloys in lightweight structures (e.g., aerospace, automotive components). This not only aligns with China's green and low-carbon development goals but also enhances the market competitiveness of magnesium alloys in the lightweight material market.

Furthermore, the LCA results also verify the rationality of the machine learning-based optimization method—by accurately optimizing the smelting parameters, the process achieves the dual goals of "stable reduction rate" and "energy conservation and emission reduction", which is more efficient and environmentally friendly than the traditional experimental optimization method. This integrated approach of "process optimization + LCA assessment" provides a new paradigm for the green optimization of magnesium smelting processes, and can also be extended to other metallurgical processes (e.g., steel smelting, aluminum smelting) to promote the low-carbon transformation of the metallurgical industry.

## 6. Conclusions

(1) The effects of varying gas flow rates, briquetting pressures, ferrosilicon content, reduction temperatures, and reduction times on the magnesium reduction rate were investigated.

(2) The SVM model developed for predicting the magnesium reduction rate demonstrates high accuracy, with a RMSE of less than 2.84%. The magnesium reduction rate, which is influenced by gas flow rate, briquetting pressure, reduction temperature, and reduction time, aligns with the underlying metallurgical mechanisms as predicted by the SVM model.

(3) Based on the established SVM model, an intelligent algorithm was employed to optimize the magnesium smelting process while maintaining a constant reduction rate. Compared to the original process, the optimized method features a reduced gas flow rate and a shorter reduction time, successfully achieving the goal of resource conservation.

(4) LCA assessment focusing on energy consumption and CO<sub>2</sub> emissions shows that the optimized process reduces total energy consumption by 5.33% and CO<sub>2</sub> emissions by 3.63%, argon gas consumption by 20% compared with the initial process, providing precise environmental performance data for the promotion and application of magnesium alloys in lightweight structures. This study not only provides a new method for the green optimization of magnesium smelting processes but also highlights the value of integrating ML and LCA in metallurgical process optimization, which is conducive to promoting the low-carbon development of the magnesium metallurgy industry.

---

## 7. Declaration of Competing Interest

The authors declare that they have no known competing financial interests or personal relationships that could have appeared to influence the work reported in this paper.

## 8. Acknowledgements

Authors would like to acknowledge the financial supports from Natural Science Foundation of Henan (252300421576, 252300421437, 252300421962), The Foundation of He'nan Educational Committee (25A430026), the China Postdoctoral Science Foundation (Grant No. 2025M770230), the Zhengzhou University of Light Industry Doctoral Research Initiation Fund (2024BSJJ003), Key Scientific and Technological Project of Henan Province (242102231007), National Natural Science Foundation of China (52475172) and Major Science and Technology Projects of Longmen Laboratory (NO.231100220400).

## 9. Author contributions

Xin Li: conceptualization, investigation, writing - original draft, writing - review and editing, and visualisation. Junhua Guo: experimental work, supervision, visualization and validation. Jianglei Fan, Yongbiao Wang: technical support and resources. Yanyan Li: technical support and help with energy consumption calculation. Xiaoguang Zhou, Shuxia Tian: technical support and help with optimization algorithm. Feng Mao, Kunlin Miao: technical support and help with XRD characterisation. Shizhong Wei: technical support and visualisation.

## 10. Data Availability Statement

Data will be made available on request.

## 11. References

- [1] W.J. Joost, P.E. Krajewski, Towards magnesium alloys for high-volume automotive applications, *Scripta Materialia*, 128 (2017) 107–112. <https://doi.org/10.1016/j.scriptamat.2016.07.035>.
- [2] A. Maqbool, N.Z. Khan, A.N. Siddiquee, Towards Mg based light materials of future: properties, applications, problems, and their mitigation, *Journal of Manufacturing Science and Engineering*, 144 (3) (2022) 030801. <https://doi.org/10.1115/1.4051678>.
- [3] T. Kurzynowski, A. Pawlak, I. Smolina, The potential of SLM technology for

- 
- processing magnesium alloys in aerospace industry, *Archives of Civil and Mechanical Engineering*, 20 (1) (2020) 23. <https://doi.org/10.1007/s43452-020-00033-1>.
- [4] D.D. Zhang, F. Peng, X.Y. Liu, Protection of magnesium alloys: from physical barrier coating to smart self-healing coating, *Journal of Alloys and Compounds*, 853 (2021) 157010. <https://doi.org/10.1016/j.jallcom.2020.157010>.
- [5] Z.Z. Yin, W.C. Qi, R.C. Zeng, X.B. Chen, C.D. Gu, S.K. Guan, Y.F. Zheng, Advances in coatings on biodegradable magnesium alloys, *Journal of Magnesium Alloys*, 8 (1) (2020) 42–65. <https://doi.org/10.1016/j.jma.2019.09.008>.
- [6] W.J. Botta, G. Zepon, T.T. Ishikawa, D.R. Leiva, Metallurgical processing of Mg alloys and MgH<sub>2</sub> for hydrogen storage, *Journal of Alloys and Compounds*, 897 (2022) 162798. <https://doi.org/10.1016/j.jallcom.2021.162798>.
- [7] Q.C. Yu, Y. Deng, S.B. Yin, Z.Y. Li, Thermal process for magnesium production with Al-Si-Fe from coal fly ash: thermodynamics and experimental investigation, *Journal of Mining and Metallurgy, Section B: Metallurgy*, 57 (3) (2021) 421–430. <https://doi.org/10.2298/JMMB210118038Y>.
- [8] J. Du, W. Han, Y. Peng, Life cycle greenhouse gases, energy and cost assessment of automobiles using magnesium from Chinese Pidgeon process, *Journal of Cleaner Production*, 18 (2) (2010) 112–119. <https://doi.org/10.1016/j.jclepro.2009.08.013>.
- [9] Y.S. Che, G.P. Mai, S.J. Zhang, J.L. He, J.X. Song, J.H. Yi, Kinetic mechanism of magnesium production by silicothermic reduction of CaO·MgO in vacuum, *Transactions of Nonferrous Metals Society of China*, 30 (10) (2020) 2812–2822. [https://doi.org/10.1016/S1003-6326\(20\)65423-1](https://doi.org/10.1016/S1003-6326(20)65423-1).
- [10] Y. Tian, L.P. Wang, B. Yang, Y.N. Dai, B.Q. Xu, F. Wang, N. Xiong, Comparative evaluation of energy and resource consumption for vacuum carbothermal reduction and Pidgeon process used in magnesium production, *Journal of Magnesium Alloys*, 10 (3) (2022) 697–706. <https://doi.org/10.1016/j.jma.2020.09.024>.
- [11] M. Abdellatif, Review of the development work on the Mintek thermal magnesium process (MTMP), *Journal of the South African Institute of Mining and Metallurgy*, 111 (6) (2011) 393–399. <https://www.saimm.co.za/Journal/v111n06p393.pdf>.
- [12] C. Zhang, C. Wang, S.J. Zhang, L.J. Guo, Experimental and numerical studies on a one-step method for the production of Mg in the silicothermic reduction process, *Industrial & Engineering Chemistry Research*, 54 (36) (2015) 8883–8892. <https://doi.org/10.1021/acs.iecr.5b01830>.
- [13] D.X. Fu, T.A. Zhang, Z.H. Dou, L.K. Guan, A new energy-efficient and environmentally friendly process to produce magnesium, *Canadian Metallurgical Quarterly*, 56 (4) (2017) 418–425. <https://doi.org/10.1080/00084433.2017.1361178>.
- [14] Y. Wada, S. Fujii, E. Suzuki, M.M. Maitani, S. Tsubaki, S. Chonan, M. Fukui, N. Inazu, Smelting magnesium metal using a microwave Pidgeon method, *Scientific Reports*, 7 (1) (2017) 46512. <https://doi.org/10.1038/srep46512>.
- [15] N. Xiong, Y. Tian, D. Yang, B.Q. Xu, T. Dai, Y.N. Dai, Results of recent investigations of magnesia carbothermal reduction in vacuum, *Vacuum*, 160 (2019)

- 
- 213–225. <https://doi.org/10.1016/j.vacuum.2018.11.007>.
- [16] B.A. Chubukov, S.C. Rowe, A.W. Palumbo, M.A. Wallace, A.W. Weimer, Investigation of continuous carbothermal reduction of magnesia by magnesium vapor condensation onto a moving bed of solid particles, *Powder Technology*, 365 (2020) 2–11. <https://doi.org/10.1016/j.powtec.2019.01.067>.
- [17] J.H. Guo, D.X. Fu, J.B. Han, Z.H. Ji, Z.H. Dou, T.A. Zhang, Kinetics of extracting magnesium from prefabricated pellets by silicothermic process under flowing argon atmosphere, *Journal of Mining and Metallurgy, Section B: Metallurgy*, 56 (3) (2020) 379–386. <https://doi.org/10.2298/JMMB200712031G>.
- [18] J.H. Guo, X. Li, T.A. Zhang, J.B. Han, J.Y. Geng, Y.S. Wang, Comparison of extraction behavior of magnesium from magnesite/magnesia by aluminothermic process in flowing argon, *Journal of Sustainable Metallurgy*, 8 (2022) 1756–1768. <https://doi.org/10.1007/s40831-022-00604-x>.
- [19] J.B. Han, D.X. Fu, J.H. Guo, Z.H. Ji, T.A. Zhang, Volatilization and condensation behavior of magnesium vapor during magnesium production via a silicothermic process with magnesite, *Vacuum*, 189 (2021) 110227. <https://doi.org/10.1016/j.vacuum.2021.110227>.
- [20] S.H. Farjana, N. Huda, M.A.P. Mahmud, R. Saidur, A review on impact of mining and mineral processing industries through life cycle assessment, *Journal of Cleaner Production*, 231 (2019) 1200–1217. <https://doi.org/10.1016/j.jclepro.2019.05.264>.
- [21] Y.T. Wang, C.Y. Zhang, Y. Rezgui, A. Ghoroghi, Z.W. Luo, Y.J. Li, T.Y. Zhao, From buildings to district: A systematic review of life cycle assessment approaches for energy system planning and optimization, *Building and Environment*, 295 (2026) 114441. <https://doi.org/10.1016/j.buildenv.2026.114441>.
- [22] Y.L. Liu, C. Niu, Z. Wang, Y. Gan, Y. Zhu, S. Sun, T. Shen, Machine learning in materials genome initiative: A review, *Journal of Materials Science & Technology*, 57 (2020) 113–122. <https://doi.org/10.1016/j.jmst.2020.01.067>.
- [23] C.G. Shen, C.C. Wang, X.L. Wei, Y. Li, S.V.D. Zwaag, W. Xu, Physical metallurgy-guided machine learning and artificial intelligent design of ultrahigh-strength stainless steel, *Acta Materialia*, 179 (2019) 201–214. <https://doi.org/10.1016/j.actamat.2019.08.033>.
- [24] X. Li, Q.M. Jiang, X.G. Zhou, G.M. Cao, G.D. Wang, Z.Y. Liu, Machine learning complex interactions among recovery, precipitation, and recrystallization for Nb micro-alloyed steels, *Metals and Materials International*, 30 (1) (2023) 167–181. <https://doi.org/10.1007/s12540-023-01493-9>.
- [25] X.F. Wang, F. Mao, X. Li, K.L. Miao, R.X. Shi, Y.C. Lin, C. Chen, C.J. Wang, H. Yu, S.Z. Wei, Machine learning-based prediction of microstructure and mechanical properties for 12Cr2Mo1V large cylindrical forgings, *Materials Today Communications*, 47 (2025) 112983. <https://doi.org/10.1016/j.mtcomm.2025.112983>.
- [26] Y. Zhong, F. Mao, X. Li, K.L. Miao, R.X. Shi, B.N. Yu, C. Chen, C.J. Wang, H. Yu, S.Z. Wei, Prediction of mechanical properties of 16Mn large tube plates based on machine learning, *Materials Today Communications*, 49 (2025) 113712. <https://doi.org/10.1016/j.mtcomm.2025.113712>.

- 
- [27] Y.F. Wen, C.Z. Cai, X.H. Liu, J.F. Pei, X.J. Zhu, T.T. Xiao, Corrosion rate prediction of 3C steel under different seawater environment by using support vector regression, *Corrosion Science*, 51 (2009) 349-355. <https://doi.org/10.1016/j.corsci.2008.10.038>.
- [28] X. Li, Q.M. Jiang, X.G. Zhou, S.W. Wu, G.M. Cao, Z.Y. Liu, Machine learning interphase precipitation behavior of Ti micro-alloyed steel guided by physical metallurgy principle, *Journal of Materials Research and Technology*, 25 (2023) 2641–2653. <https://doi.org/10.1016/j.jmrt.2023.06.077>.
- [29] L. Wu, F. Han, G. Liu, *Magnesium smelting via the Pidgeon process*, Springer, Singapore, 2021, p.45-68.

JMMB – accepted – manuscript

---

A separate list of figures captions

Fig. 1 The flowchart of machine learning.

Fig. 2 Phase analysis of ferrosilicon.

Fig. 3 Schematic diagram of flowing argon atmosphere magnesium smelting theory.

Fig. 4 Comparison between predicted and measured magnesium reduction rate in training and testing datasets.

Fig. 5 The influence of gas flow rate and briquetting pressure on magnesium reduction rate.

Fig. 6 Effects of reduction temperature and reduction time on magnesium reduction rate.

Fig. 7 Effects of ferrosilicon content on magnesium reduction rate.

Table 1 Chemical composition of ferrosilicon alloy.

Table 2 Theoretical calculation of ingredients.

Table 3 Comparison of initial and optimized magnesium smelting processes.

JMMB – accepted – manuscript